06.1;06.5;13.1;13.3;15.2

Multiple variations in the electrical capacitance of laser-induced graphene with varying synthesis modes

© K.G. Mikheev, R.G. Zonov, D.L. Bulatov, A.V. Syugaev, G.M. Mikheev

Udmurt Federal Research Center, Ural Branch of Russian Academy of Sciences, Izhevsk, Russia
E-mail: mikheev@udman.ru

Received April 27, 2024
Revised June 10, 2024
Accepted June 22, 2024

Laser-induced graphene (LIG) is a graphene-like highly porous electrically conductive film-type material synthesized by laser pyrolysis of a carbon-containing dielectric material. This paper reports on the findings regarding the influence of the LIG synthesis modes on its electrical capacitance. Synthesis of LIG was carried out by line-by-line scanning of a cw CO_2 laser beam over the polyimide film surface; electrical capacitance of the obtained samples was determined by the two-electrode cyclic voltammetry in the sulfuric acid solution. It was found out that, by reducing the laser beam scanning speed and adjusting the laser power, it is possible to increase the LIG specific capacitance from 2.6 to 27 mF/cm^2.

Keywords: laser pyrolysis, polyimide film, scanning speed, electrical capacitance.

DOI: 10.61011/TPL.2024.10.60118.19976

Laser-induced graphene (LIG) is a three-dimensional porous graphene. It may be obtained by laser pyrolysis of an appropriate precursor in the open air atmosphere without creating special conditions. LIG is regarded as a very attractive material for various applications [1]. The most effective precursor for the LIG synthesis is a polyimide film (PF) on the surface of which a flexible film structure with reproducible parameters may be obtained [2]. LIG has a highly developed surface and relatively low surface resistance [3], which allows using it as a basis for designing and constructing various devices and sensors [4,5], as well as microsupercapacitors (MSCs) [6]. When LIG is placed in an electrolyte solution, the electrode/electrolyte interfaces get charged with formation of a double electrical layer whose capacitance determines the MSC capacitance [7]. The important parameters that significantly affect electrical capacitance of such MSCs are thickness of the synthesized carbon material [8], specific surface area, pore size and distribution [6,9], concentration of free charge carriers, and water wettability [10,11]. Those parameters may be managed by varying the LIG synthesis modes (see, e.g. [12–14]). Recently there have been published a large number of papers devoted to studying conditions for synthesizing LIG with various lasers. Despite the availability of some individual papers [15], there are no systematic studies aimed at searching for the LIG synthesis modes involving low-power cw CO_2 lasers in order to obtain MSCs with high electrical capacitance.

The goal of this work was to study the modes of laser pyrolysis of PF with a cw carbon-dioxide laser in view of obtaining high capacitance LIG.

In the experiments, the LIG film structure was formed on a 200 μm thick PF as a result of line-by-line scanning of its surface with a focused beam of the cw CO_2 laser. The laser beam diameter on the film surface was $d = 120\,\mu$m, while the interline distance was $\Delta = 25\,\mu$m. The LIG film structure was formed at different laser powers (P) for fixed values of scanning speed v being varied from 10 to 300 mm/s.

Capacitive properties of the prepared LIG samples were studied by the two-electrode cyclic voltammetry (CV) in the 1 M aqueous solution of H_2SO_4 by using a potentiostat-galvanostat. For this purpose, on the PF there was fabricated a pair of identical LIG film samples 10×10 mm in size with 8×8 mm contact pads (see the inset in Fig. 1, a) necessary for attaching the current collectors. The LIG specific capacitance (c) was measured immediately after submerging the samples in the electrolyte and also after soaking them in the electrolyte for 12 h. In the experiments, the dependence of specific capacitance c on laser power P was examined at various preset laser beam scanning speeds v.

Fig. 2, a demonstrates a typical scanning electron microscopy (SEM) image of the LIG surface. One can see that the structure obtained is a highly porous spongy material. Fig. 2, b presents a typical LIG Raman spectrum measured with a spectrometer with the 632.8 nm excitation radiation. The spectrum consists of a luminescent background and four main features D, G, D' and $2D$ that are characteristic of multilayer graphene nanocrystallites [16]. Peak frequencies of those bands are 1330, 1581, 1615 and 2661 cm^{-1}, respectively. The experiments have shown that, when $v = \text{const}$, ratios I_{2D}/I_G and I_D/I_G indicating the graphenization degree and defect density, respectively [17], depend complexly on P (insets in Fig. 2, b).

Fig. 3, a presents stabilized CV curves for three LIG samples synthesized at different P for $v = 120$ mm/s. The curves were measured on the samples pre-soaked

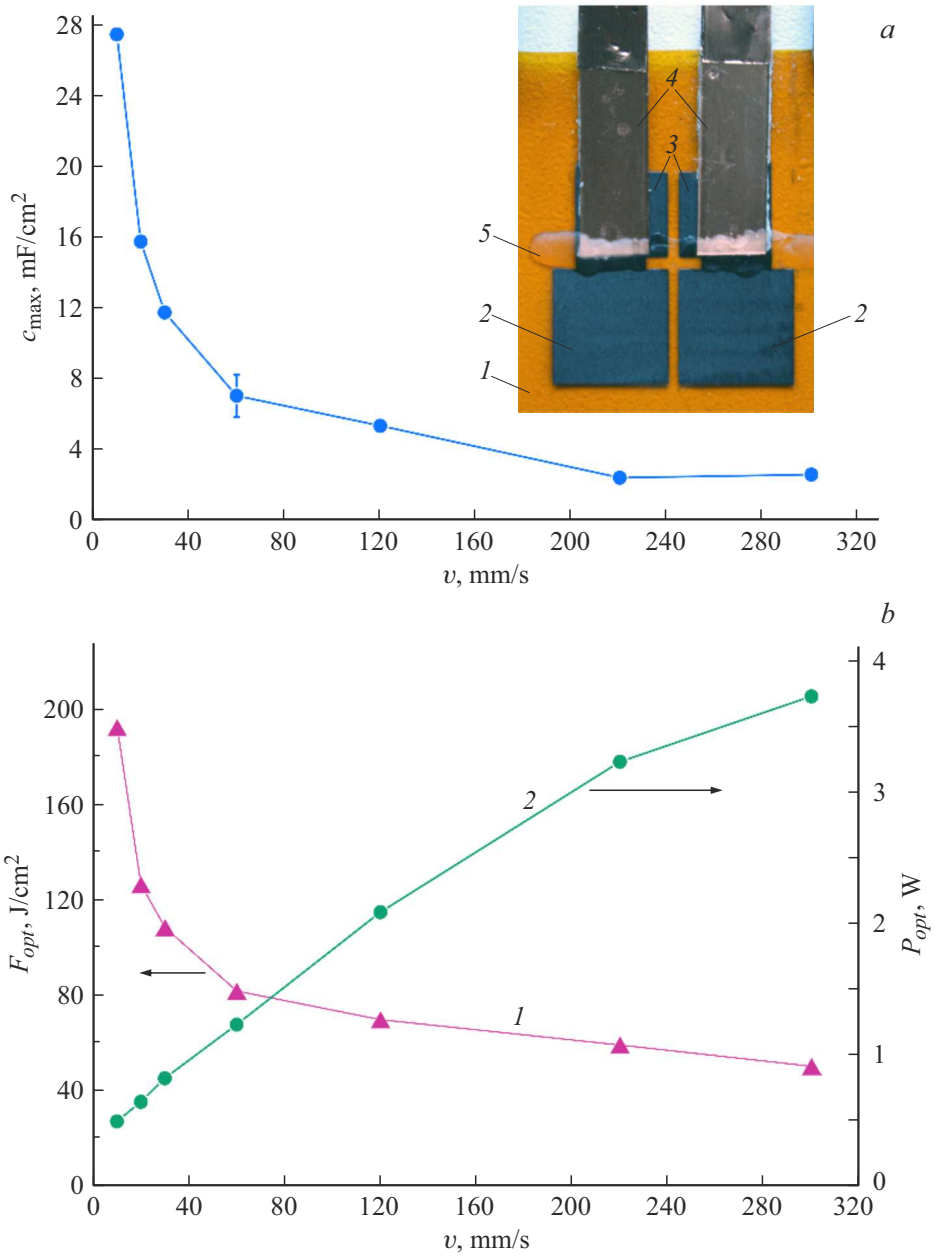


Figure 1. *a* — maximal specific capacitance c_{max} as a function of scanning speed v and a photograph (in the inset) of a pair of LIG samples prepared for measurements in the electrolyte solution. *1* — polyimide film, *2* — LIG 10×10 mm, *3* — contact pad 8×8 mm, *4* — copper/film current collector, *5* — paraffin barrier. *b* — optimal energy density F_{opt} (*1*) and optimal power P_{opt} (*2*) versus scanning speed v.

in electrolyte at the potential sweep rate of 20 mV/s. Areas under the curves are directly proportional to specific capacitance c defined as $c = q/U_{max}$, where q is the operating capacitor plate charge measured by the potentiostat at voltage $U_{max} = 1$ V. Fig. 3, *a* clearly shows that the areas under the CV curves depend significantly on the power of the laser used in the LIG synthesis. Fig. 3, *b* demonstrates the $c(P)$ dependences for samples synthesized at $v = 120$ mm/s, which were measured before and after soaking the samples in electrolyte. This shows that specific capacitance of all the samples synthesized at different laser powers becomes considerably higher after soaking. The obtained curves presented in Fig. 3, *b* are similar to each other, which may be caused by the identity of surface areas occupied by pores which get impregnated not immediately after submerging the sample in the electrolyte but after 12 h. The figure also shows that at fixed speed $v = 120$ mm/s there exists optimal laser power $P_{opt} = 2.1$ W at which maximum specific capacitance values $c_{max} = 3.8$ and 5.3 mF/cm^2 get achieved before and

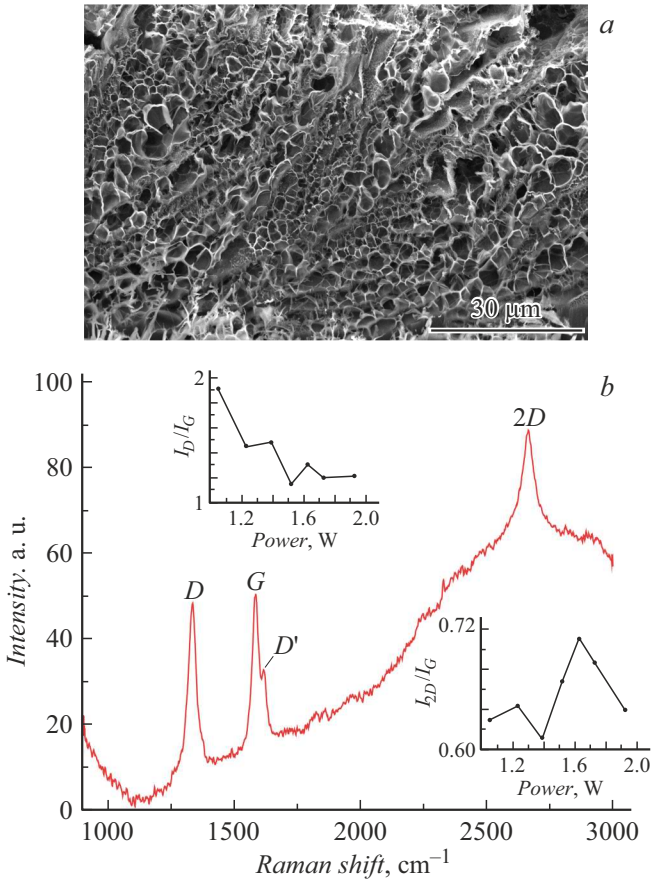


Figure 2. A typical SEM image of the LIG surface (a) and typical LIG Raman spectrum recorded with the helium-neon laser excitation at the wavelength of 632.8 nm (b). The insets present the dependences of ratios I_D/I_G and I_{2D}/I_G on the laser power, which were obtained at scanning speed $v = 80$ mm/s.

after soaking, respectively. P_{opt} corresponds to the optimal absorbed energy density F_{opt} defined as $F_{opt} = P_{opt}/(v\Delta)$ in the case of the line-by-line laser synthesis of LIG with neglected reflected radiation [15]. Numerous measurements gave dependences $c_{\max}(v)$, $P_{opt}(v)$ and $F_{opt}(v)$ presented in Fig. 1. An increase in $c_{\max}$ and F_{opt} and decrease in P_{opt} with decreasing scanning speed are clearly seen. The maximum capacitance is 2.6 mF/cm^2 at $v = 300$ mm/s ($P_{opt} = 3.7$ W) and $c_{\max} = 27$ mF/cm^2 at $v = 10$ mm/s ($P_{opt} = 0.5$ W). Worth noting, at $v < 10$ mm/s, a solid LIG film allowing for electrochemical studies could hardly be obtained. Notice also that specific capacitance of LIG synthesized by the PF pyrolysis with a repetitively pulsed CO_2 laser is 1.2–3.9 mF/cm^2 [4,12], while its maximum value achieved in the case of using a cw CO_2 laser was $c = 22.2$ mF/cm^2 [15]. The $c_{\max}$ increase with a decrease in v may be explained by an increase in the specific surface area S_{sa} and LIG mass M_{LIG} per unit of its visible surface s, i. e. parameter M_{LIG}/s. The S_{sa} values measured by the BET (Brunauer–Emmett–Teller) method for $v = 10$ mm/s ($P_{opt} = 0.5$ W) and $v = 300$ mm/s ($P_{opt} = 3.7$ W) were 330 and 180 m^2/g, respectively, while parameter M_{LIG}/s corresponding for those modes was equal to 1 and 0.26 mg/cm^2, respectively. An increase in the specific surface area of pores S_{sa} and in parameter M_{LIG}/s by 1.83 and 3.8 times leads to the 7 fold increase in the total surface area of all the LIG pores per s, which is accompanied by a multiple increase in $c_{\max}$. Based on the values of M_{LIG}/s and $c_{\max}$, it is possible to determine gravimetric specific electrical capacitance c_g; it appeared to be 10 and 27.6 F/g for $v = 10$ mm/s ($P_{opt} = 0.5$ W) and $v = 300$ mm/s ($P_{opt} = 3.7$ W), respectively. Papers [2] and [4] give for LIG synthesized on PF by using a repetitively pulsed CO_2 laser the c_g values of 120 and

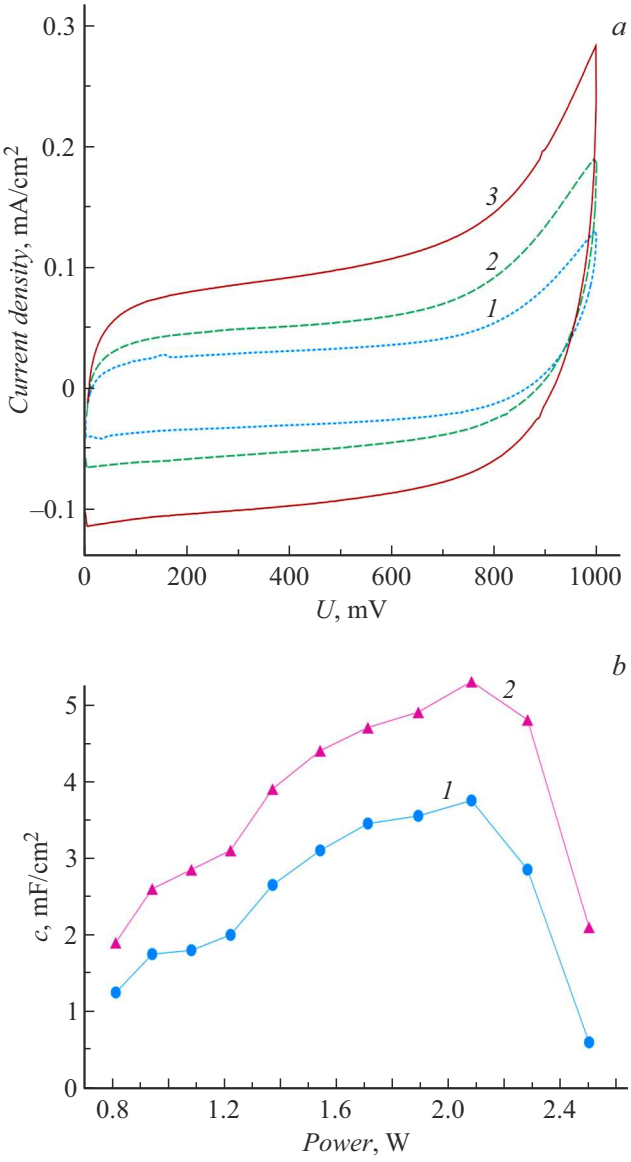


Figure 3. a — stabilized CV characteristics of LIG samples synthesized at scanning speed $v = 120$ mm/s and laser powers $P = 0.8$ (*1*), 1.2 (*2*) and 2.1 W (*3*). b — specific capacitance c of LIG samples synthesized at $v = 120$ mm/s versus laser power P before (*1*) and after (*2*) sample soaking in the 1 M solution of H_2SO_4 for 12 h.

65 F/g, respectively (in [4], the data was obtained after special modification of pre-synthesized LIG).

Thus, this study has shown experimentally for the first time that, in the process of laser pyrolysis of PF by line-by-line scanning with the cw CO_2 laser beam, the synthesized LIG capacitance increases significantly with decreasing scanning speed due to an increase in the material specific surface area and mass per unit surface.

Acknowledgements

The experiments were conducted at the facilities of CUC of the Udmurt Federal Research Center (Ural Branch of RAS).

Funding

The study was accomplished under State Assignment of the RF Ministry of Science and Higher Education (State Registration Number 1021032422167-7-1.3.2 and FUUE-2024-0011).

Conflict of interests

The authors declare that they have no conflict of interests.

References

[1] Y. Guo, C. Zhang, Y. Chen, Z. Nie, Nanomaterials, **12**, 2336 (2022). DOI: 10.3390/nano12142336
[2] J. Lin, Z. Peng, Y. Liu, F. Ruiz-Zepeda, R. Ye, E.L.G. Samuel, M.J. Yacaman, B.I. Yakobson, J.M. Tour, Nat. Commun., **5**, 5714 (2014). DOI: 10.1038/ncomms6714
[3] K.G. Mikheev, R.G. Zonov, N.V. Chuchkalov, G.M. Mikheev, Phys. Solid State, **66** (2), 268 (2024). DOI: 10.61011/PSS.2024.02.57924.5.
[4] W. Zhang, Q. Jiang, Y. Lei, H.N. Alshareef, ACS Appl. Mater. Interfaces, **11**, 20905 (2019). DOI: 10.1021/acsami.9b05635
[5] Z. Yin, S. Chen, C. Hu, J. Li, X. Ang, Opt. Laser Technol., **176**, 110998 (2024). DOI: 10.1016/j.optlastec.2024.110998
[6] M. Reina, A. Scalia, G. Auxilia, M. Fontana, F. Bella, S. Ferrero, A. Lamberti, Adv. Sustain. Syst., **6**, 2100228 (2022). DOI: 10.1002/adsu.202100228
[7] K.G. Mikheev, A.V. Syugaev, R.G. Zonov, D.L. Bulatov, G.M. Mikheev, Phys. Solid State, **65** (2), 347 (2023). DOI: 10.21883/PSS.2023.02.55422.529.
[8] X. Yu, N. Li, S. Zhang, C. Liu, L. Chen, S. Han, Y. Song, M. Han, Z. Wang, J. Power Sources, **478**, 229075 (2020). DOI: 10.1016/j.jpowsour.2020.229075
[9] A.V. Syugaev, R.G. Zonov, K.G. Mikheev, A.N. Maratkanova, G.M. Mikheev, J. Phys. Chem. Solids, **181**, 111533 (2023). DOI: 10.1016/j.jpcs.2023.111533
[10] Z. Peng, R. Ye, J.A. Mann, D. Zakhidov, Y. Li, P.R. Smalley, J. Lin, J.M. Tour, ACS Nano, **9**, 5868 (2015). DOI: 10.1021/acsnano.5b00436
[11] W. Song, J. Zhu, B. Gan, S. Zhao, H. Wang, C. Li, J. Wang, Small, **14**, 1702249 (2018). DOI: 10.1002/smll.201702249
[12] R. Ye, D.K. James, J.M. Tour, Adv. Mater., **31**, 1803621 (2019). DOI: 10.1002/adma.201803621
[13] K.G. Mikheev, R.G. Zonov, A.V. Syugaev, D.L. Bulatov, G.M. Mikheev, Phys. Solid State, **64** (5), 579 (2022). DOI: 10.21883/PSS.2022.05.53520.277.
[14] J. de la Roche, I. López-Cifuentes, A. Jaramillo-Botero, Carbon Lett., **33**, 587 (2023). DOI: 10.1007/s42823-022-00447-2
[15] A. Velasco, Y.K. Ryu, A. Hamada, A. de Andrés, F. Calle, J. Martinez, Nanomaterials, **13**, 788 (2023). DOI: 10.3390/nano13050788
[16] K.G. Mikheev, R.G. Zonov, T.N. Mogileva, A.E. Fateev, G.M. Mikheev, Opt. Laser Technol., **141**, 107143 (2021). DOI: 10.1016/j.optlastec.2021.107143
[17] I.R. Hristovski, L.A. Herman, M.E. Mitchell, N.I. Lesack, J. Reich, J.F. Holzman, Nanomaterials, **12**, 1241 (2022). DOI: 10.3390/nano12081241

Translated by EgoTranslating